Supplement of Biogeosciences, 12, 4693–4709, 2015
http://www.biogeosciences.net/12/4693/2015/
doi:10.5194/bg-12-4693-2015-supplement

Supplement of

Probing the past 30-year phenology trend of US deciduous forests

X. Yue et al.

Correspondence to: X. Yue (xuyueseas@gmail.com)

Supporting Information

Derivation of phenological observations

One difficulty in analyzing trend of forest phenology is the missing of long-term records. In this study, we derive phenological observations in combination of date records, leaf area index (LAI), and photos. Date records are complete and last for >20 years at Harvard Forest and Hubbard Brook. However, the data are incomplete at US-UMB and US-MMS. Budburst dates are documented for 10 years at US-UMB (Fig. S2a). We use the LAI measurements from 1999 to gap fill the missing dates. In this procedure, the budburst dates are defined as the days when the interpolated or extrapolated LAI is equal to a selected threshold (LAIt), which may vary from 0.5 to 2.0. As shown in Fig. S2a, a different LAIt can determine an independent time series. The most reasonable LAIt is determined if the derived time series has the lowest root-mean-square error (RMSE) against the available date records. For example, the RMSE for derived phenology is 5.6 days with LAIt=1.3 m^2 m^{-2}, 3.2 days with LAIt=1.5 m^2 m^{-2}, and 4.1 days with LAIt=1.7 m^2 m^{-2}. As a result, we select LAIt = 1.5 m^2 m^{-2} as the standard threshold to derive the missing budburst dates. The same spring LAIt is applied to derive dormancy onset dates, which also show low RMSE against other sources of autumn phenology (Fig. S2b). A similar procedure is performed for US-MMS and a lower LAIt of 1.4 m^2 m^{-2} is selected for this site (Figs. S2c-S2d). As a check, we also derive phenological dates for US-Ha1 with A higher LAIt of 1.75 m^2 m^{-2} (Figs. S2e-S2f). However, for US-Ha1, date records are comprehensive while LAI measurements are incomplete and as a result we do not use the LAI-derived dates in the model validations at this site (e.g. Fig. 1).

In case that the LAI measurements are also incomplete, we derive those missing dates using photos from PhenoCam (http://phenocam.sr.unh.edu/webcam/). Different from the quantitative estimate with LAI, the derivation with photo is qualitative. We define the budburst date as the middle of the few days when tree colors change rapidly from gray to light green. On the contrary, a dormancy start date is defined as the middle of days with rapid color changes from brown to gray. An example of autumn dormancy at US-UMB is shown in Fig. S3. The comparison shows that the photo-derived dates are not largely different from the LAI-derived ones (Fig. S2b). We aggregate all the available dates to develop the most complete dataset for validation (Fig. 1). In case of data overlap from different sources, we select date records as the primary choice and that derived from LAI as the secondary.

We also derive phenological dates for the USA National Phenology Network (USA-NPN). The network has limited records before 2009 but is significantly enriched thereafter. Currently, there are >600000 records for >20000 individual plants at >6500 sites. Due to the large data amount, we select observations during 2011-2012 for 52 deciduous tree species that are the most common in the U.S. (Table S1). In total, we have records at 588 sites (Table 1); however, not all of these sites provide continuous year-round observations. We apply the following stringent screening filter to derive the phenological dates with high confidence. Each USA-NPN record reports 2-10 phenological statuses, including breaking leaf buds, >=75% of full leaf size, >=50% of leaves colored, >=50% of leaves fallen, all leaves fallen, and so on. We determine budburst date as the first day with 'breaking leaf buds' and dormancy onset as the first day with 'all leaves fallen'. To ensure that the selected date is the real 'first day' for the phenological shift, we require that there is at least one record beforehand showing no onset of the phenological events. For example, a record with true status of 'breaking leaf buds' is not used if no records in the earlier days of this year report a false status for the same event. The derived dates for individual trees are averaged among species for every site to achieve the spatial distribution of phenology.

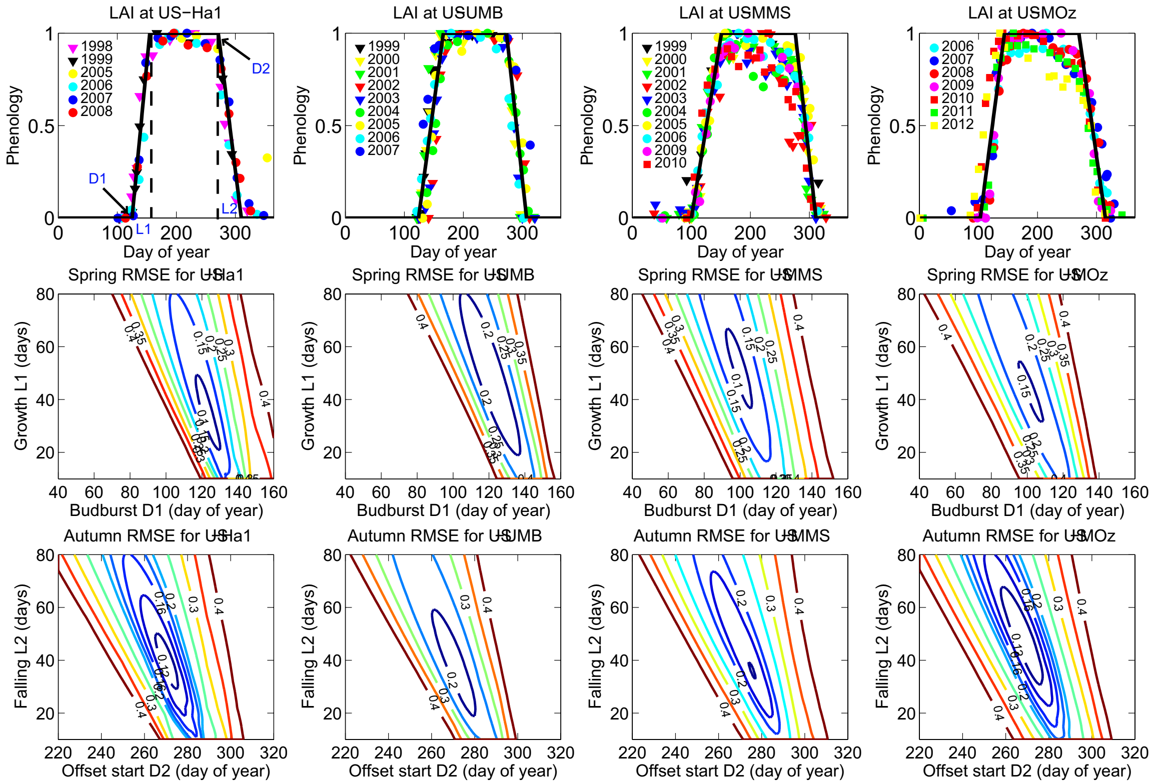

Figure S1. Observed (markers) and regressed (black lines) phenology at four DBF sites (top row). At each site, sensitivity tests of regressions for the *d*th day of the year are performed with different budburst dates (D1), growing length (L1), offset start dates (D2), and falling length (L2) as follows (marked in the top left subplot):

$$P(d)=\begin{cases}\max\left\{0,\ \min\left[(d-D1)/L1,\ 1\right]\right\}, & d\le 213\\ \max\left\{0,\ \min\left[(L2+D2-d)/L2,\ 1\right]\right\}, & d>213\end{cases}$$

The 213th day of year is correspondent to August 1st. Contour maps of the root-mean-square error (RMSE) for these regressions against observations are shown for spring (middle row) and autumn (bottom row). The optimized regressions with specific dates (D1, L1, D2, and L2), which result in a minimum regression RMSE, are shown as the bold lines in the top figures.

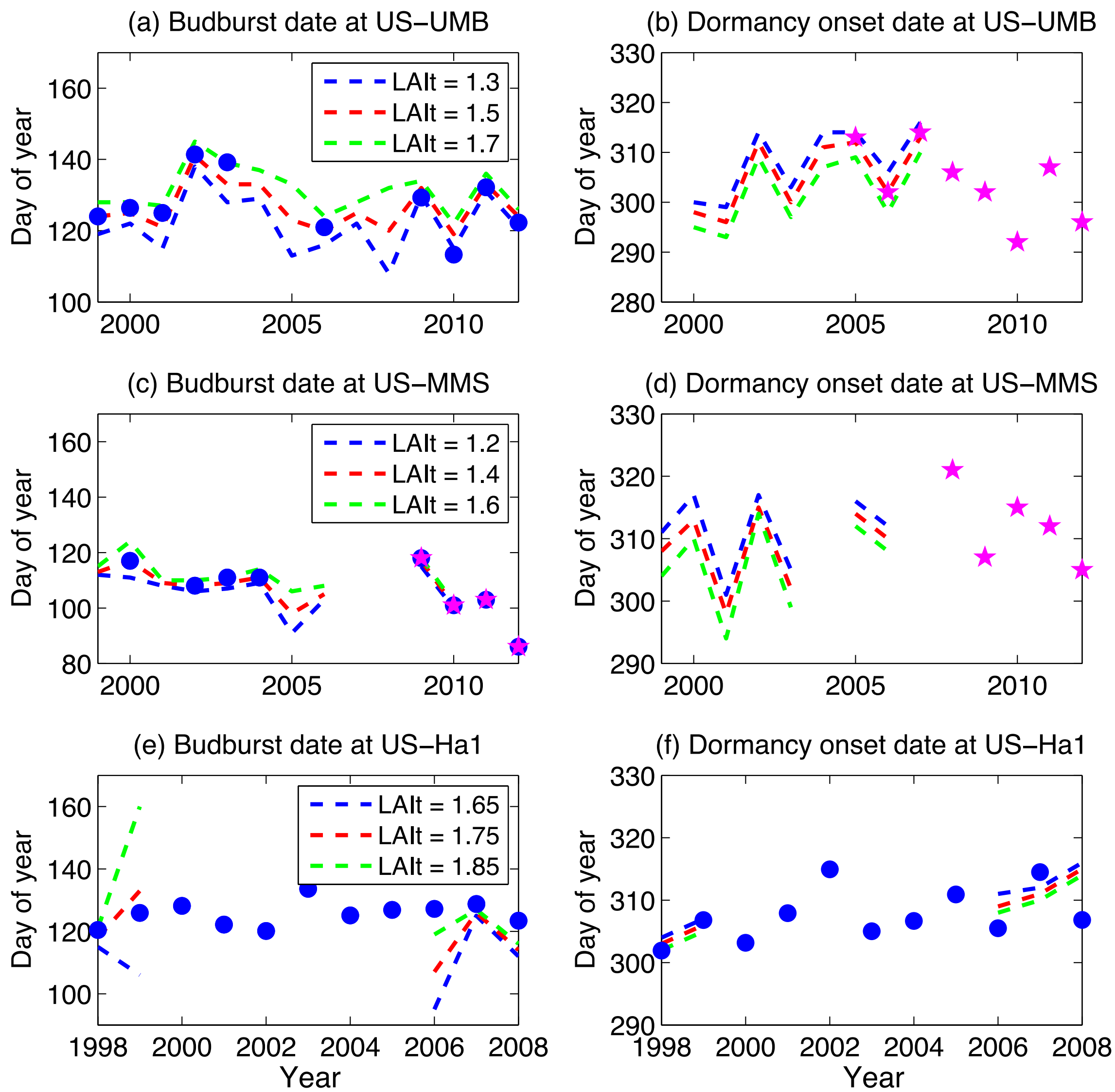

Figure S2. Derived (a, c, e) budburst and (b, d, f) dormancy onset date with different LAI thresholds at sites (a, b) US-UMB, (c, d) US-MMS, and (e, f) US-Ha1. Observations from date records are indicated as blue points. Dates derived from photos (e.g., see Fig. S3 for US-UMB) are shown as magenta pentagrams.

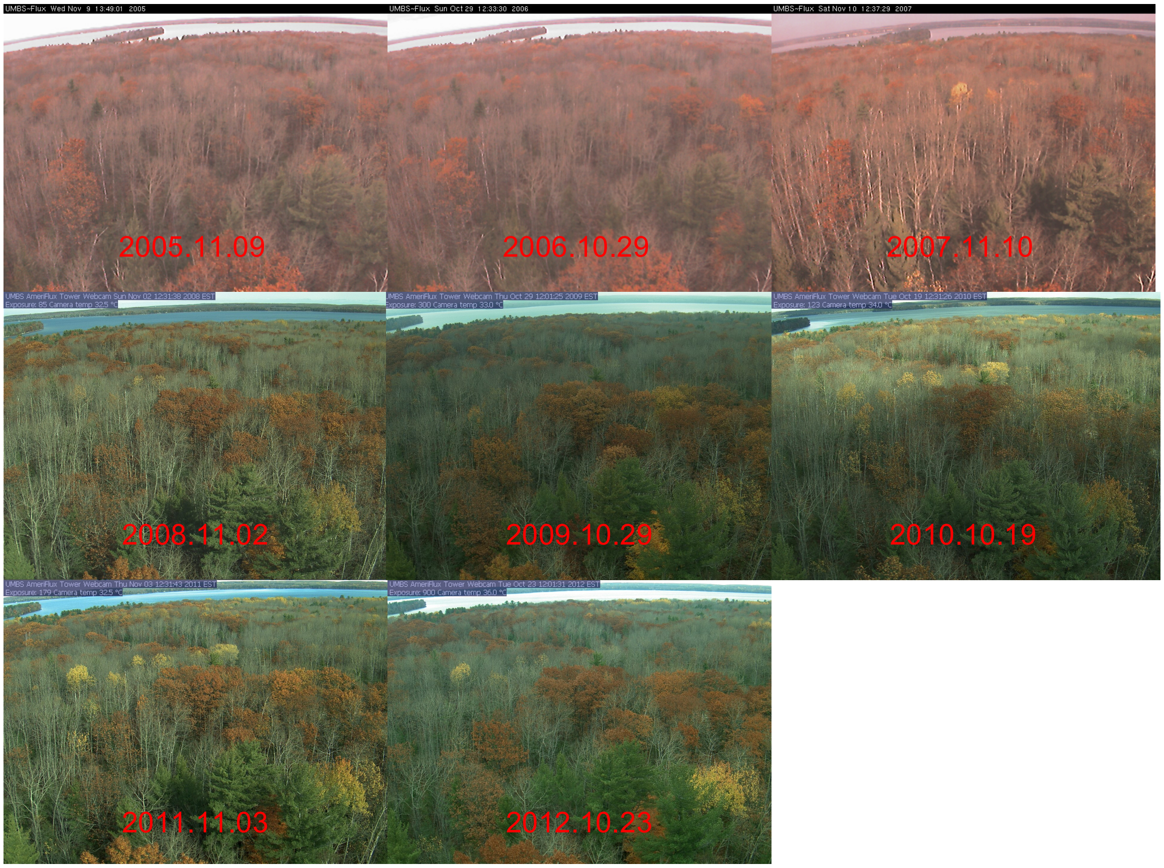

Figure S3. Photos of autumn phenology at US-UMB sites. A dormancy start date is defined as the middle of a few days with rapid color changes from brown to gray The photos after 2008 have better quality relative to earlier years due to an update of equipment.

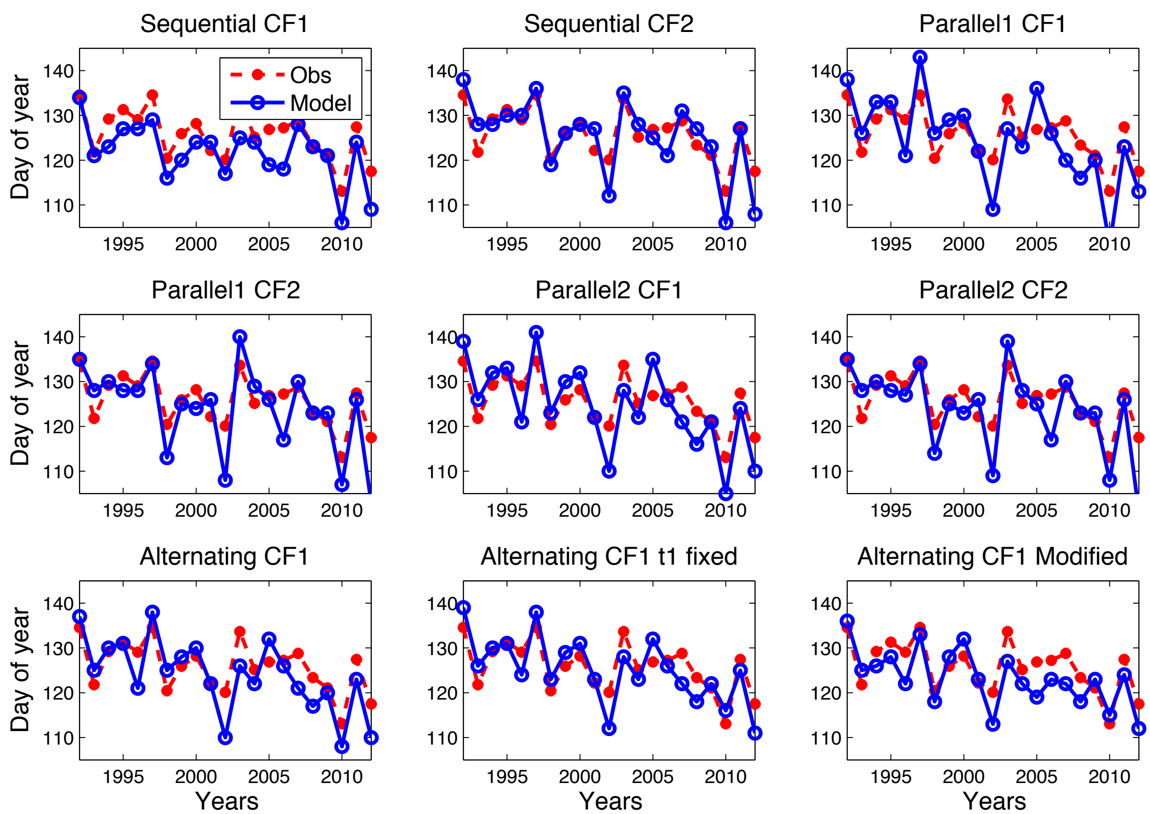

Figure S4. Comparison of predicted (blue) budburst dates at Harvard Forest with observations (red) for 1992-2012. Each panel represents results using a spring phenology model (Table 5).

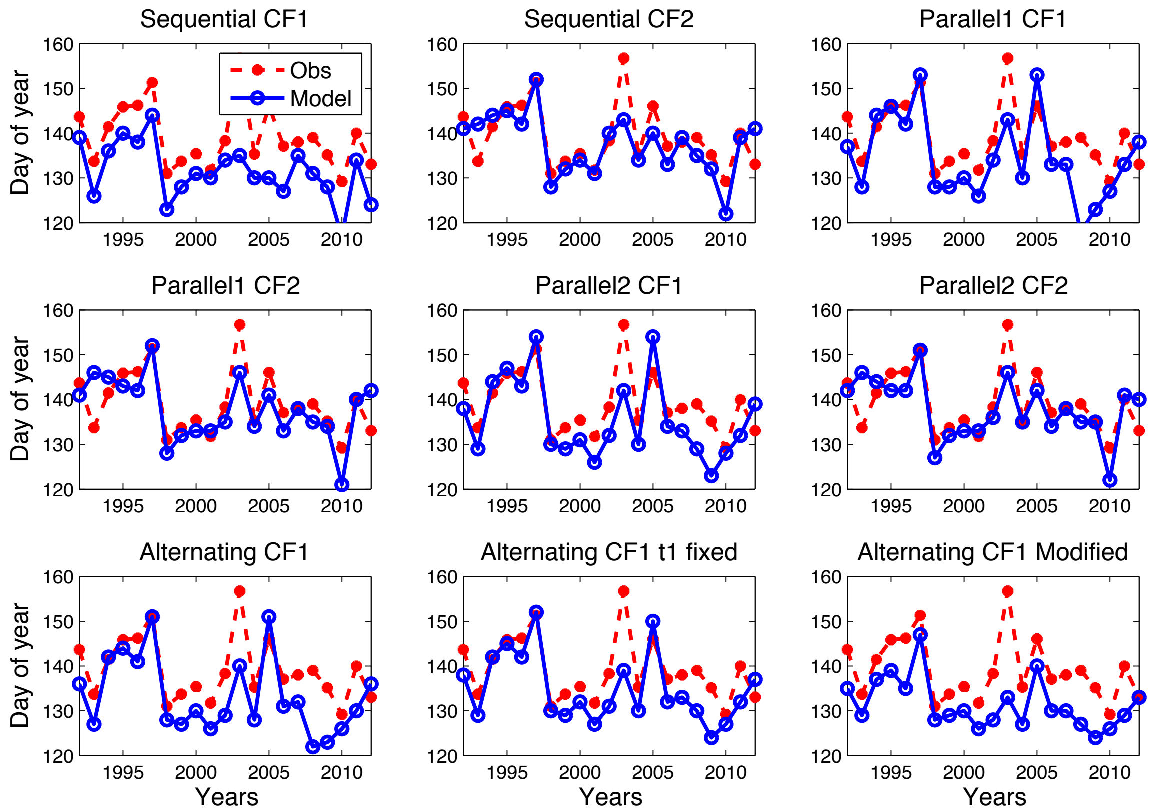

Figure S5. The same as Fig. S4 but for the site at Hubbard Brook.

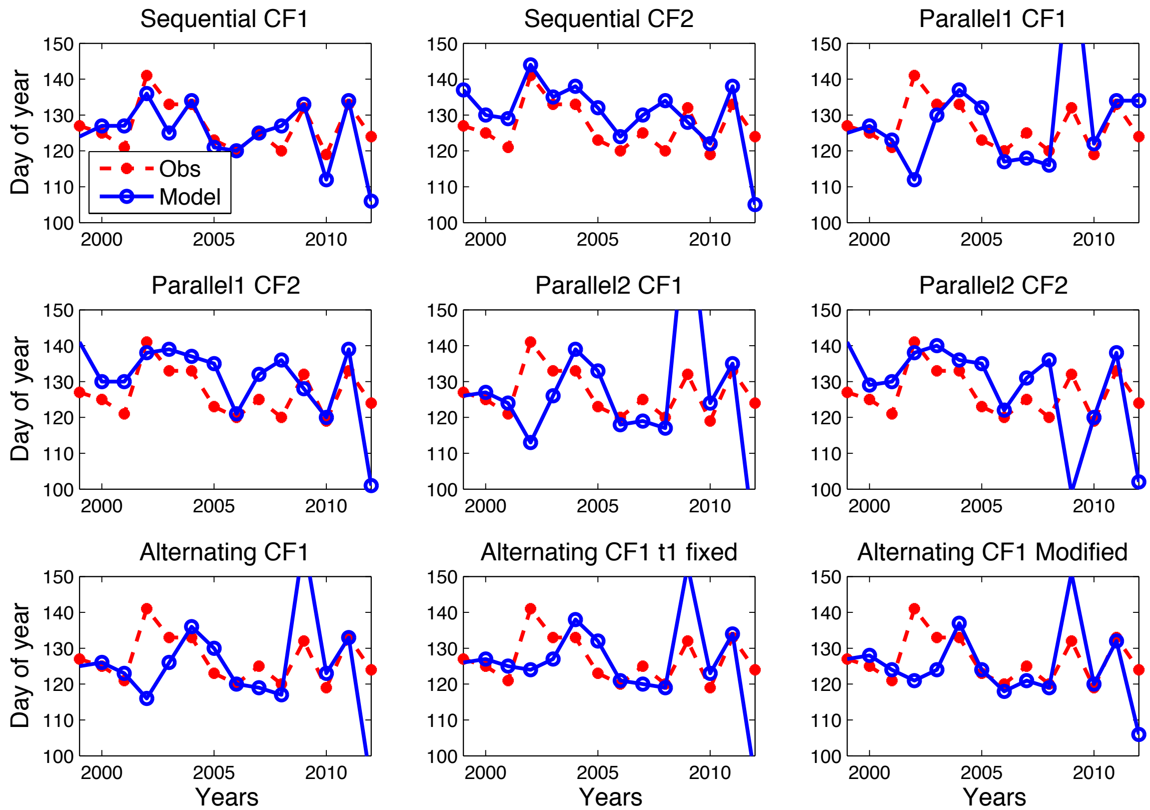

Figure S6. The same as Fig. S4 but for the site at US-UMB for 1999-2012.

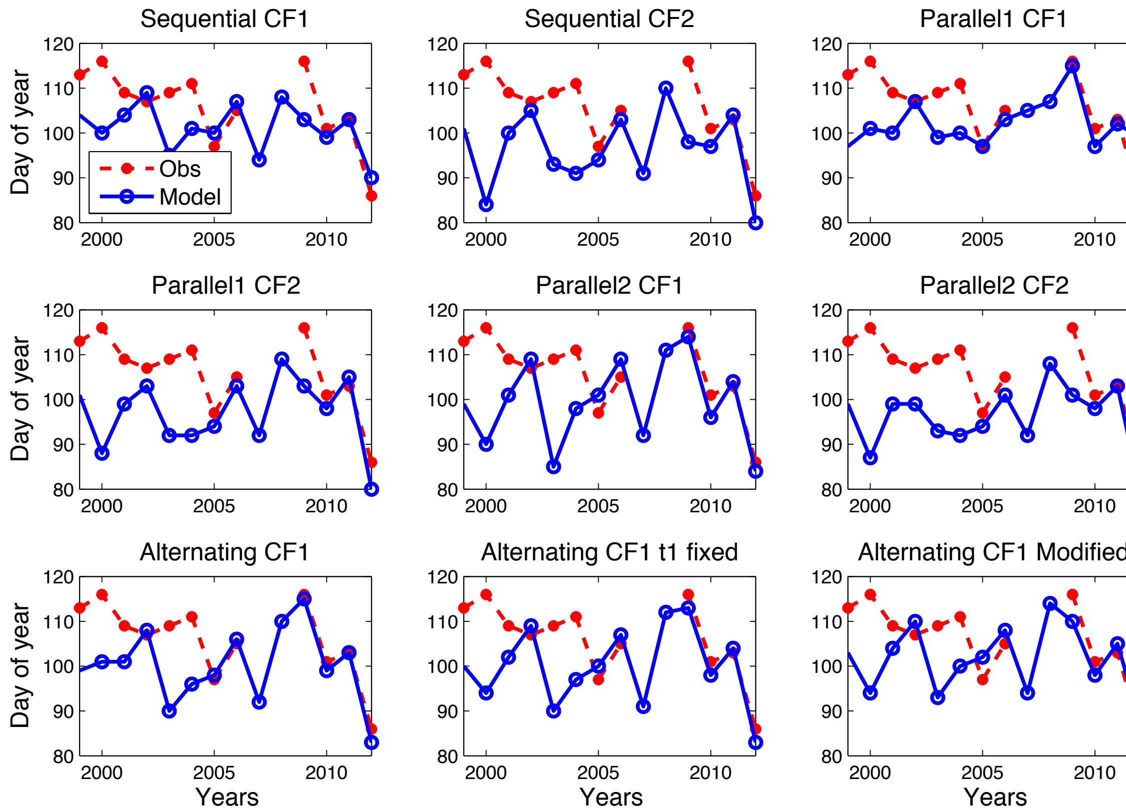

Figure S7. The same as Fig. S4 but for the site at US-MMS for 1999-2012.

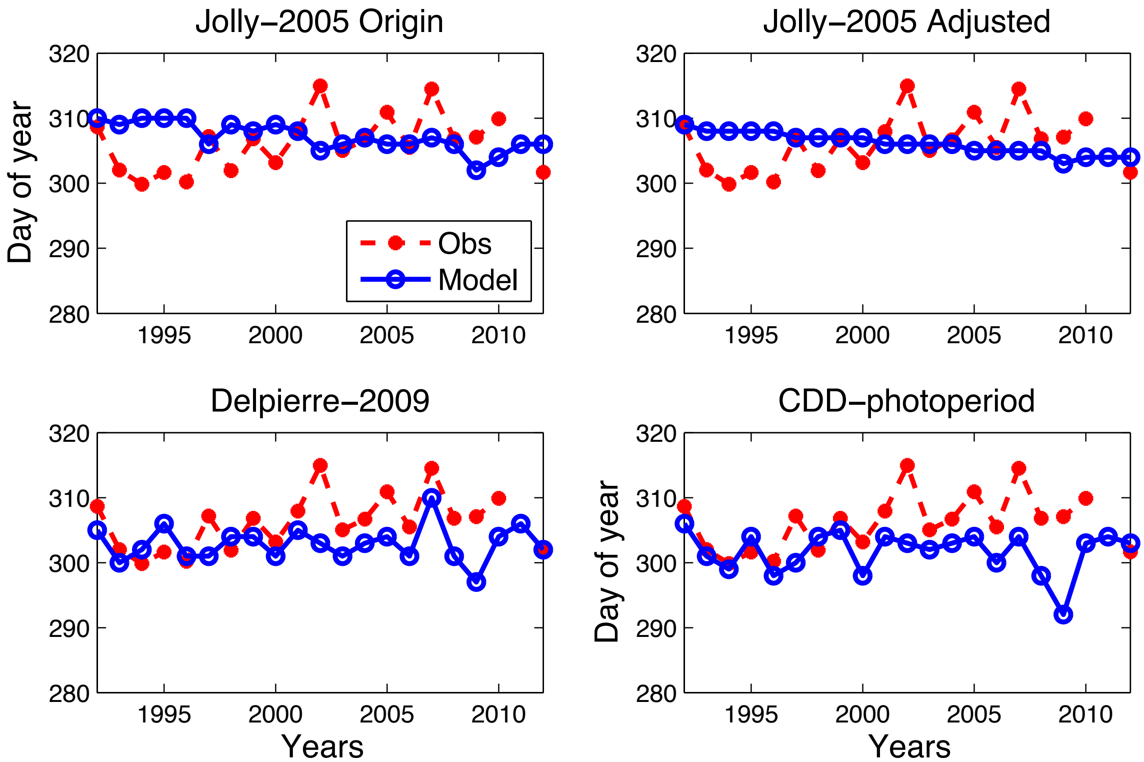

Figure S8. Comparison of predicted (blue) dormancy onset dates at Harvard Forest with observations (red) for 1992-2012. Each panel represents results using an autumn phenology model (Table 5).

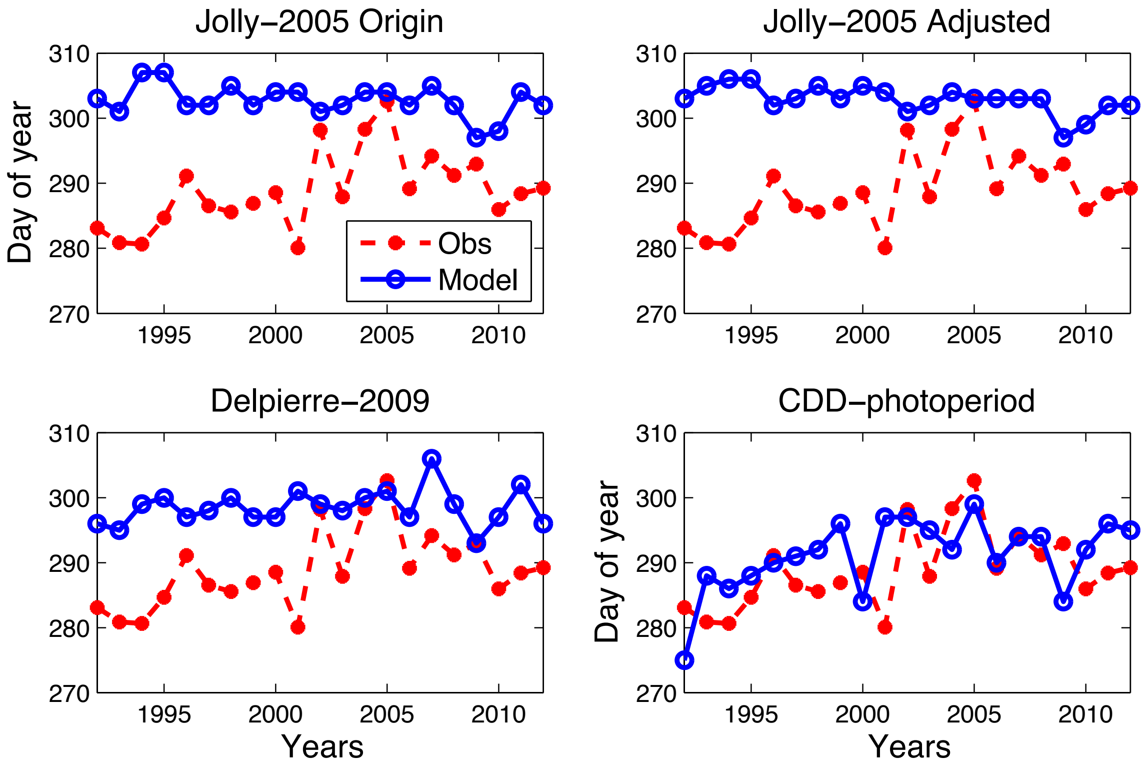

Figure S9. The same as Fig. S8 but for the site at Hubbard Brook.

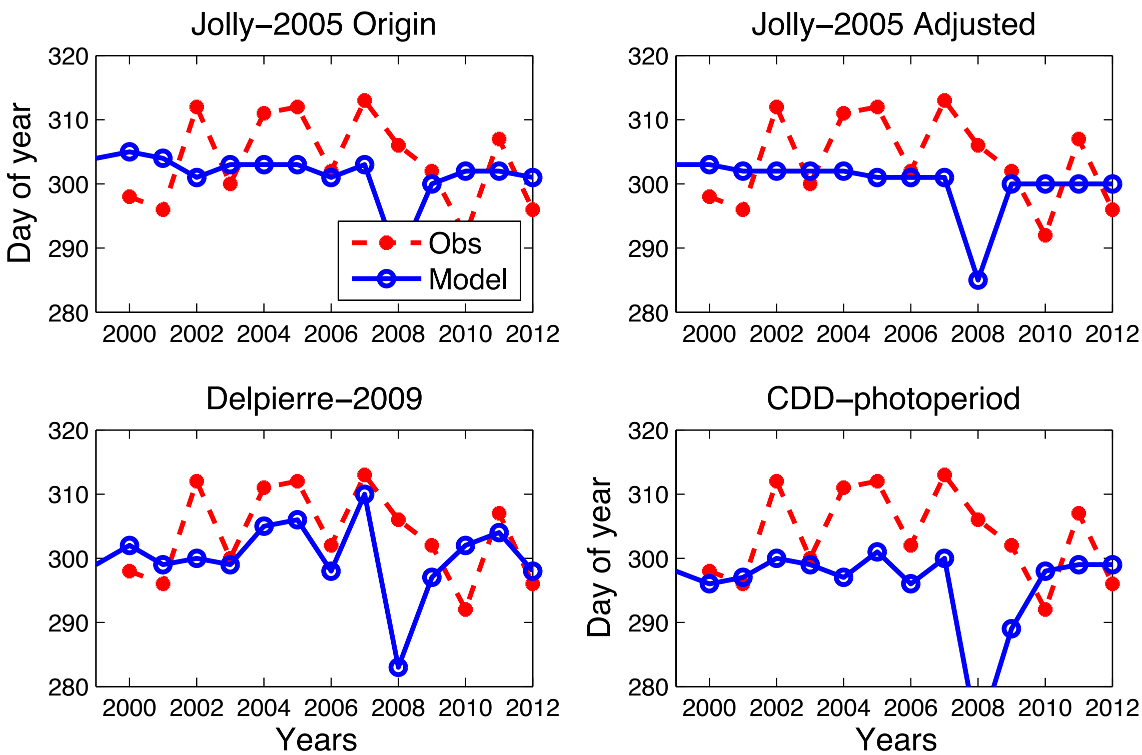

Figure S10. The same as Fig. S8 but for the site at US-UMB for 1999-2012.

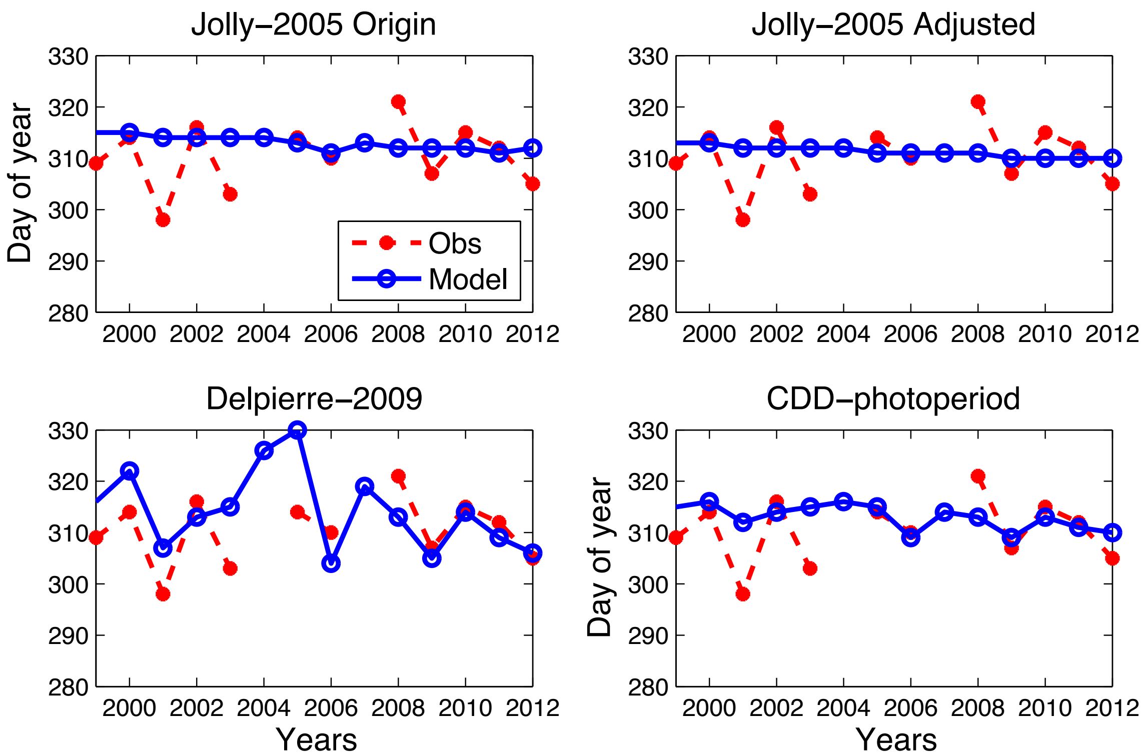

Figure S11. The same as Fig. S8 but for the site at US-MMS for 1999-2012.

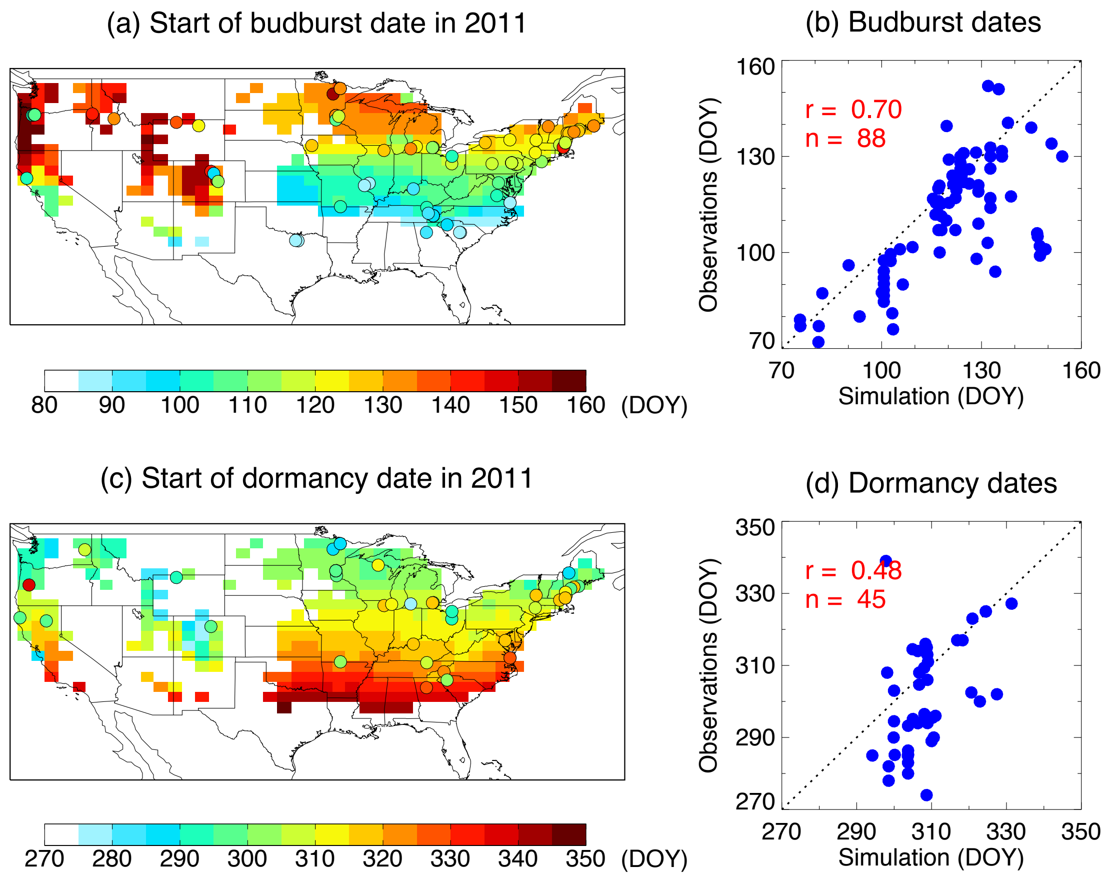

Figure S12. Comparison of the simulated (a, b) budburst and (c, d) dormancy dates with *in situ* observations (colored circles) from the USA National Phenology Network for 2011. Simulations are performed with the spring model S9 and autumn model A4. The number of the sites and the correlation coefficients are shown in the scatter plots.

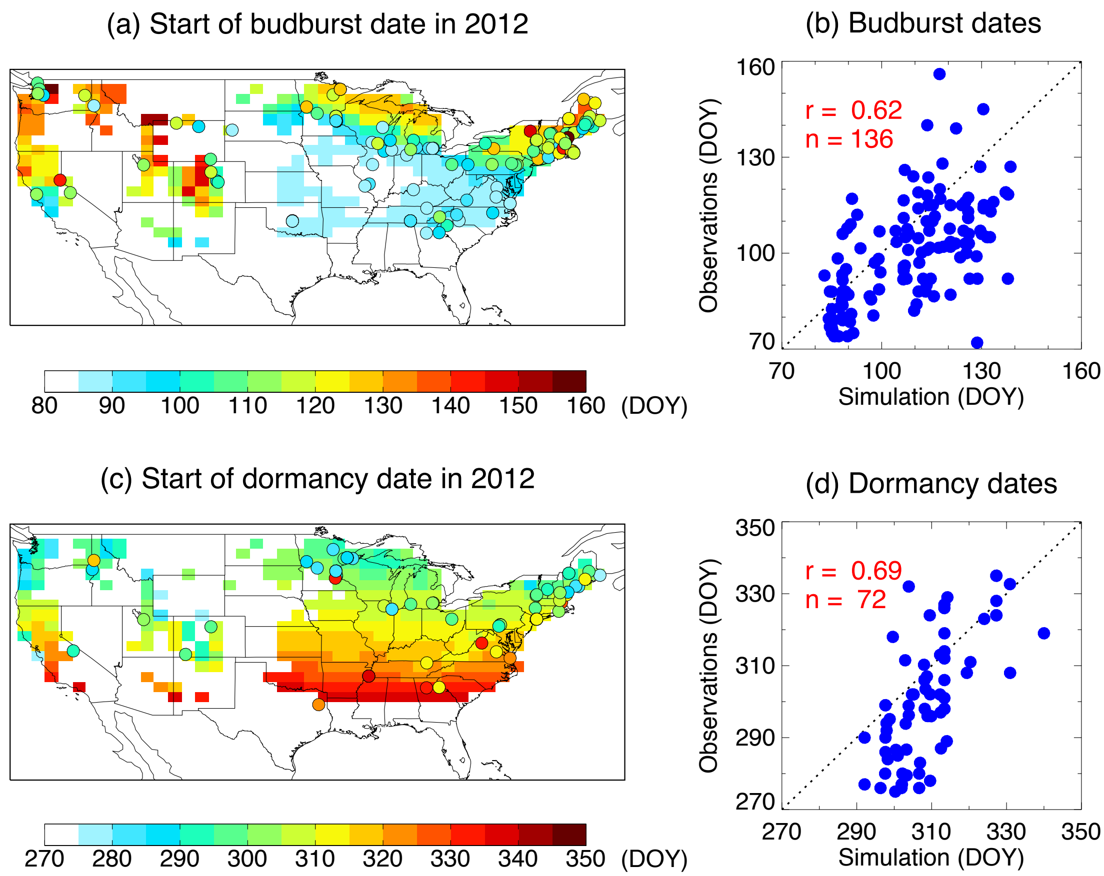

Figure S13. The same as Fig. S12 but for the year 2012.

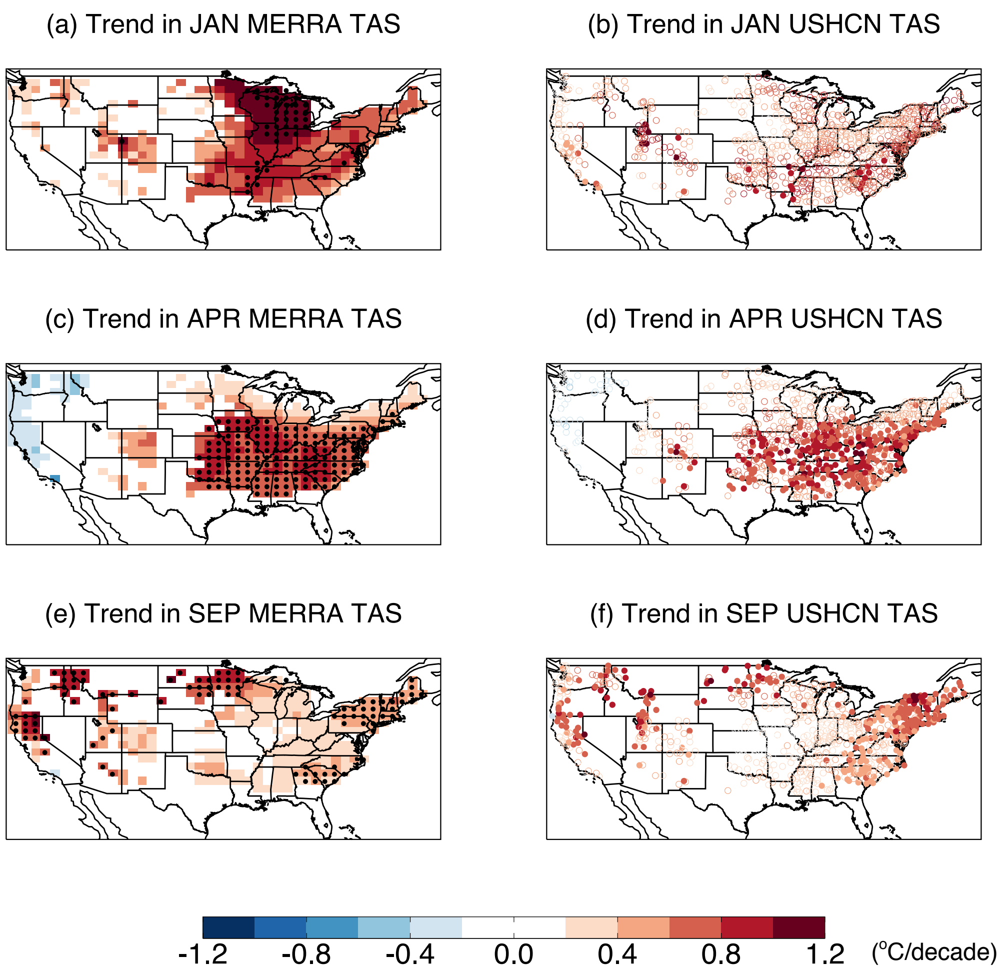

Fig. S14 Trend of surface air temperature for (a, b) January, (c, d) April, and (e, f) September over deciduous forest during 1982-2012. The temperature data are from (a, c, e) MERRA reanalyses and (b, d, f) USHCN Network. Significant trends (p<0.05) are denoted with dots (a, c, e) or filled circles (b, d, f).

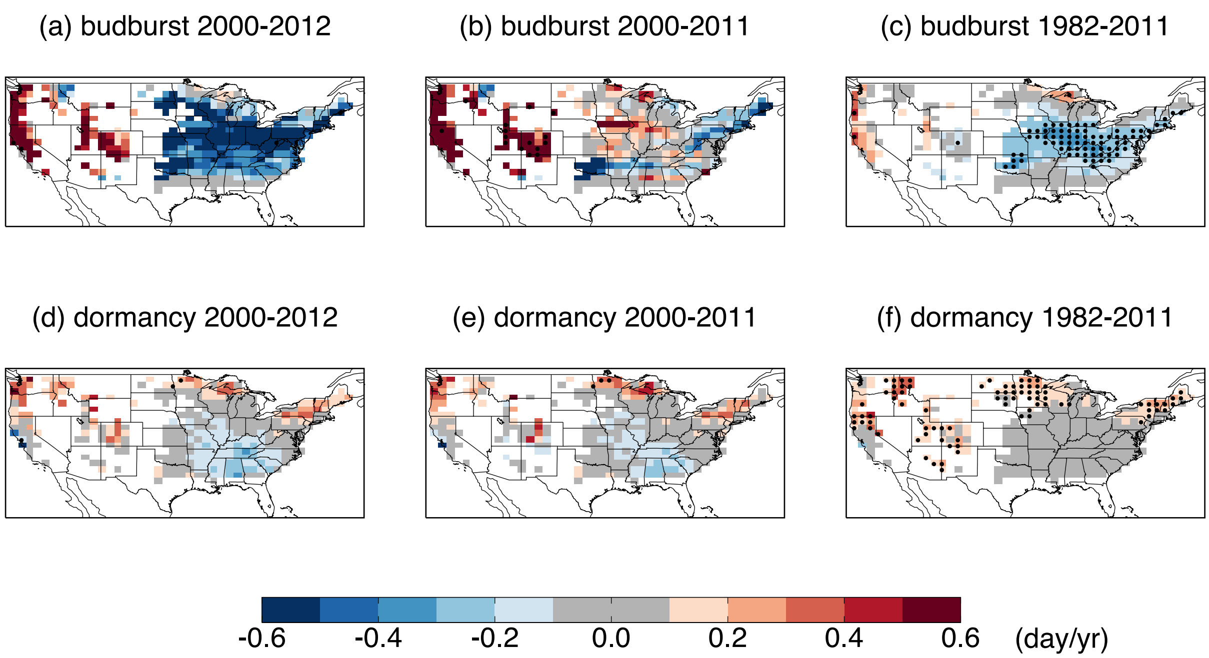

Figure S15. Trend in the simulated (a, b, c) budburst and (d, e, f) dormancy dates for deciduous forests in the U.S. during different periods. Significant trends (p<0.05) are denoted with dots.

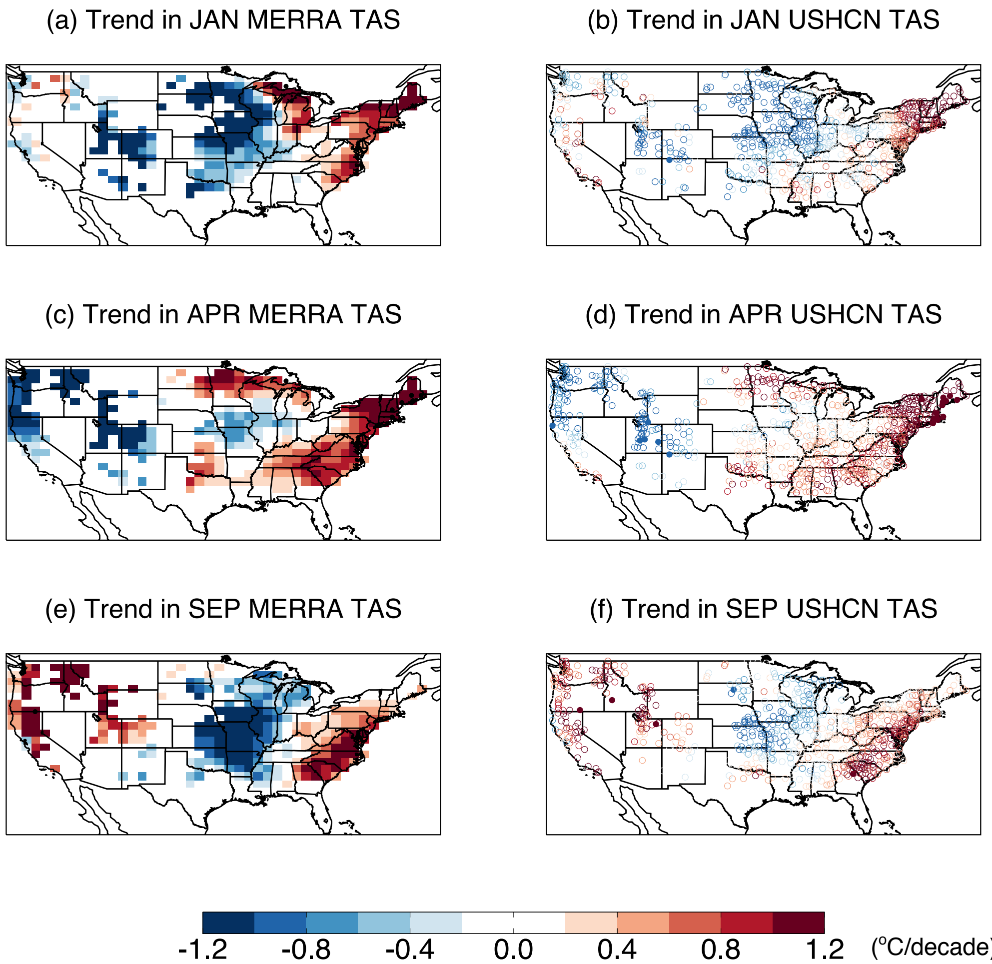

Figure S16. Trend of surface air temperature for (a, b) December, (c, d) April, and (e, f) September during 2000-2012. The temperature data are from (a, c, e) MERRA reanalyses and (b, d, f) USHCN Network. The results are shown only for the grid squares where the fraction of deciduous forest is larger than 3%. Significant trends are denoted with dots (a, c, e) or solid points (b, d, f).

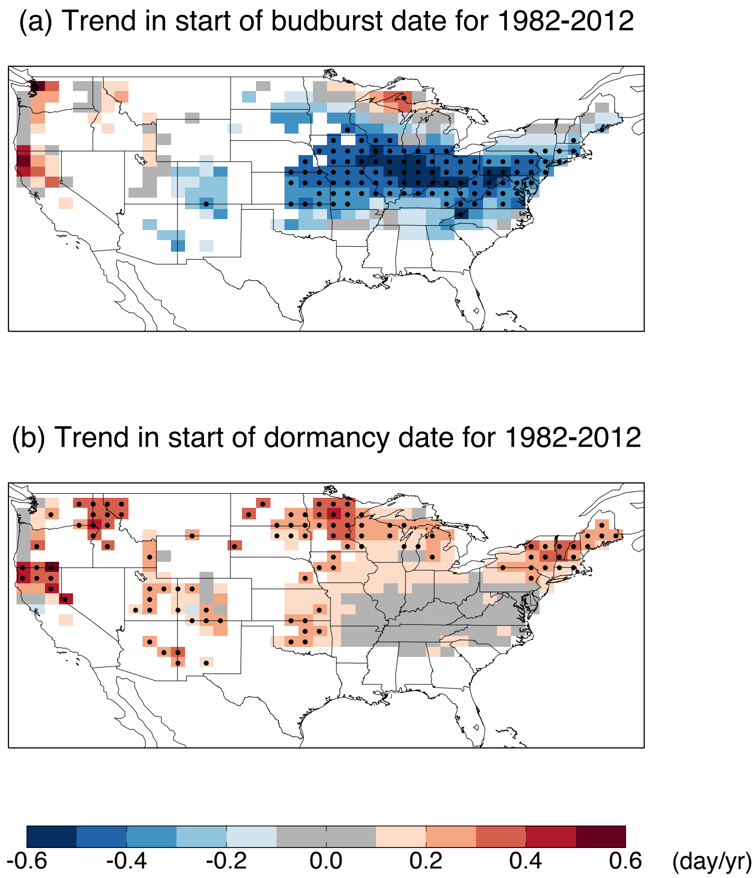

Figure S17. Trend in the simulated (a) budburst and (b) dormancy dates for deciduous forests in the U.S. during 1982-2012 using models without (a) chilling requirement and (b) photoperiod limit. The results are shown only for the grid squares where the fraction of deciduous forest is larger than 3%. Significant trends (p<0.05) are denoted with dots.

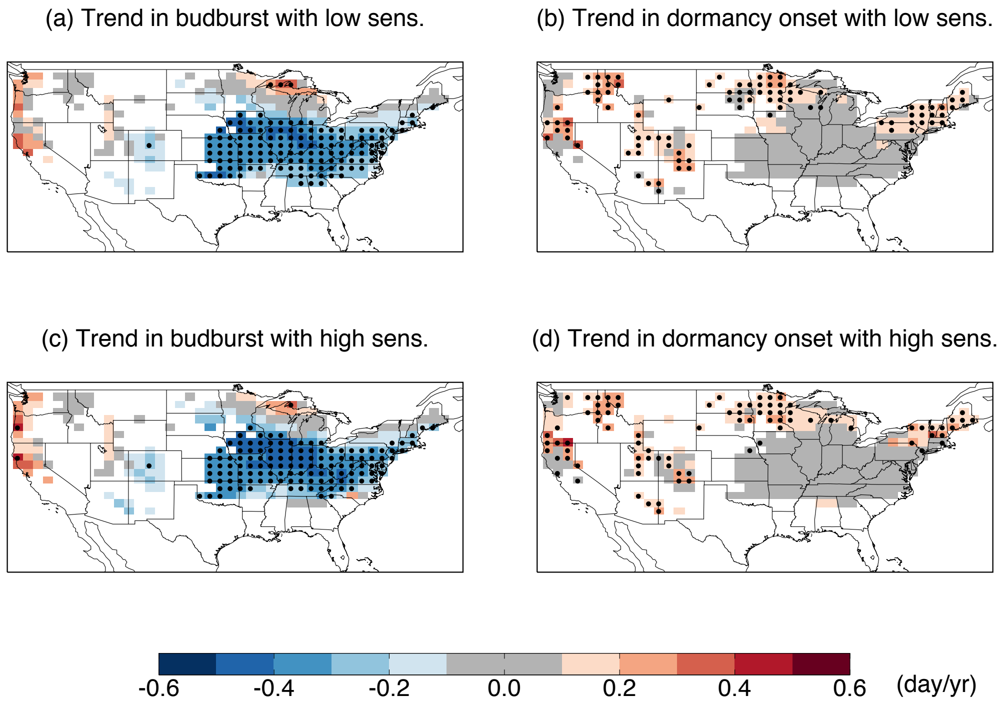

Figure S18. Trend in the simulated (a, c) budburst and (b, d) dormancy dates for deciduous forests in the U.S. during 1982-2012 using parameters derived based on phenological records of (a) Sweet Birch (*Betula Lenta*) and (c) Striped Maple (*Acer Pensylvanicum*) for spring, and (b) Paper Birch (*Betula Papyrifera*) and (d) Black Oak (*Quercus Velutina*) for autumn. The temperature sensitivity of each species is shown in Fig. 8. The results are shown only for the grid squares where the fraction of deciduous forest is larger than 3%. Significant trends (p<0.05) are denoted with dots.

Table S1. Detailed information of phenological records for 52 species from the National Phenology Network during 2011-2012.

Species	Latin Name	Common Name	Sites	Trees	Records
ACMA	Acer Macrophyllum	Bigleaf Maple	26	41	129
ACNE	Acer Negundo	Boxelder Maple	27	32	685
ACPE	Acer Pensylvanicum	Striped Maple	6	11	42
ACPL	Acer Plantanoides	Norway Maple	6	12	160
ACRU	Acer Rubrum	Red Maple	177	306	4239
ACSA1	Acer Saccharinum	Silver Maple	11	14	154
ACSA2	Acer Saccharum	Sugar Maple	75	123	1652
AEFL	Aesculus Flava	Yellow Buckeye	3	17	327
ALRU	Alnus Rubra	Red Alder	13	14	163
AMLA	Amerlanchier Laevis	Serviceberry	2	3	58
BEAL	Betula Alleghaniensis	Yellow Birch	16	39	301
BELE	Betula Lenta	Sweet Birch	9	13	86
BEPA	Betula Papyrifera	Paper Birch	38	63	1226
CACA	Carpinus Caroliniana	American Hornbeam	11	40	142
CAGL	Carya Glabra	Pignut Hickory	13	28	492
CAIL	Carya Illinoinensis	Pecan	14	36	217
CAOV	Carya Ovata	Shagbark Hickory	5	7	45
CECA	Cercis Canadensis	Redbud	60	94	1574
CEOC	Celtis Occidentalis	Hackberry	11	40	243
COFL	Cornus Florida	Flowering Dogwood	85	115	1193
DIVI	Diospyros Virginiana	Persimmon	12	17	262
FAGR	Fagus Grandifolia	American Beech	37	59	1458
FRAM	Fraxinus Americana	White Ash	12	16	135
FRPE	Fraxinus Pennsylvanica	Green Ash	20	38	489
GIBI	Ginkgo Biloba	Ginkgo	5	10	81
GLTR	Gleditsia Triacanthos	Honey Locust	8	15	101
HAVI	Hamamelis Virginia	Witch Hazel	17	26	280
ILVE	Ilex Verticillata	Winterberry	2	3	57
JUNI	Juglans Nigra	Black Walnut	27	48	579
LIST	Liquidambar Styraciflua	Sweetgum	33	55	511
LITU	Liriodendron Tulipifera	Tuliptree	44	89	716
NYSY	Nyssa Sylvatica	Black Gum	9	16	156
OXAR	Oxydendrum Arboreum	Sourwood	3	5	26
PLOC	Platanus Occidentalis	Sycamore	4	5	24
PODE	Populus Deltoides	Eastern Cottonwood	7	7	54
POTR	Populus Tremuloides	Trembling Aspen	75	135	3410
PRAM	Prunus Americana	American Plum	16	16	136
PRSE	Prunus Serotina	Black Cherry	43	73	1582
QUAL	Quercus Alba	White Oak	40	59	1158

QUMA	Quercus Macrocarpa	Bur Oak	23	38	549
QUPA	Quercus Palustris	Pin Oak	7	9	33
QURU	Quercus Rubra	Red Oak	45	57	1191
QUVE	Quercus Velutina	Black Oak	5	6	65
RHCA	Rhamnus Cathartica	Common Buckthorn	5	5	121
RHGL	Rhus Glabra	Smooth Sumac	2	2	111
ROPS	Robinia Pseudoacacia	Black Locust	14	19	362
SAAL	Sassafras Albidum	Sassafras	5	5	69
SAPU	Sambucus Pubens	Red Elderberry	8	16	781
TIAM	Tilia Americana	American Basswood	17	21	553
ULAM	Ulmus Americana	American Elm	13	34	236
VACO	Vaccinium Corymbosum	Highbush Blueberry	12	25	737
VIAL	Viburnum Alnifolium	Hobblebush	2	4	129

Table S2. Detailed information of phenological records for 7 species from the National Phenology Network during 2004-2012.

Species	Latin Name	Common Name	Trees	Records	Start	End
SYCH	Syringa Chinensis	Red Rothomagensis lilac	68	1770	2004	2012
SYVU	Syringa Vulgaris	Common Lilac	108	1581	2004	2012
LOTA	Lonicera Tatarica-arnoldred	Arnold Red honeysuckle	13	725	2004	2012
FOSP	Forsythia Spp	Forsythia	2	38	2005	2010
COCA	Cornus Canadensis	Bunchberry Dogwood	1	34	2006	2012
ACRU	Acer Rubrum	Red Maple	1	56	2006	2012
COFL	Cornus Florida	Flowering Dogwood	2	27	2007	2012

Table S3. Parameters for the phenology models (S9+A4) selected for the regional simulations.

Variables	Description	Units	Value	Reference
		Spring model S9		
t_1	Starting day for spring accumulation	DOY	356	Fixed
T_c	Base temperature for budburst forcing	°C	5	Murray et al. (1989)
a	Parameters for budburst threshold G_b	Degree day	-110	Calibrated
b	Parameters for budburst threshold G_b	Degree day	550	Calibrated
r	Parameters for budburst threshold G_b	Dimensionless	-0.01	Murray et al. (1989)
L_g	Growing length constraint	Degree day	380	Calibrated
		Autumn model A4		
t_3	Starting day for autumn accumulation	DOY	173	Fixed
T_b	Base temperature for senescence forcing	°C	20	Dufrene et al. (2005)
F_s	Threshold for leaf fall	Degree day	140	Calibrated
L_f	Falling length constraint	Degree day	410	Calibrated
P_x	Daylength threshold for leaf fall	Minutes	695	Calibrated
P_i	Daylength threshold for full dormancy	Minutes	585	Calibrated

Table S4. Summary of calibrated parameters for all phenology models except for S9 and A4. A variable is dimensionless if no units are indicated.

ID	Parameters
	Spring models
S1	t_1 = Dec 23rd, T_f = 15 °C, T_c = 0 °C, C^* = 85 days, F^* = 230 degree days
S2	t_1 = Jan 10th, T_c = -2 °C, C^* = 17, F^* = 137
S3	t_1 = Jan 8th, T_f = 9 °C, T_c = 20 °C, C^* = 85 days, a = 42 degree days, b=-0.01
S4	t_1 = Jan 10th, T_c = -3 °C, C^* = 16, a = 202, b=-0.01
S5	t_1 = t_2 = Dec 16th, T_f = 8 °C, T_c = 4 °C, C^* = 105 days, a = 77 degree days, b=-0.01
S6	t_1 = t_2 = Jan 10th, T_c = -3 °C, C^* = 21, a = 205, b=-0.01
S7	t_1 = t_2 = Jan 3rd, T_f = T_c = 8 °C, a = 590 degree days, b=-0.03
S8	t_1 = t_2 = Dec 22nd, T_f = T_c = 7 °C, a = 430 degree days, b=-0.02
	Autumn models
A1	T_i = -2 °C, T_x = 5 °C, P_i = 600 minutes, P_x = 660 minutes
A2	T_i = -1 °C, T_x = 1 °C, P_i = 600 minutes, P_x = 690 minutes
A3	P_{start} = 700 minutes, T_b = 25 °C, x = 1, y = 2, Y_{crit} = 20, L_f =402

Table S5. Summary of correlation coefficients, RMSE, the Akaike Information Criterion (AIC) for the evaluation of different spring models and autumn models.

Models	Correlation Coefficient	RMSE	AIC
	Spring Models		
S1	0.74 ± 0.13 [a]	6.14 ± 1.60	75.45 ± 13.67
S2	0.64 ± 0.20	8.71 ± 3.64	76.87 ± 6.91
S3	0.65 ± 0.16	8.41 ± 3.67	90.71 ± 10.05
S4	0.63 ± 0.15	9.46 ± 4.22	85.32 ± 8.29
S5	0.66 ± 0.14	8.85 ± 4.45	90.67 ± 10.20
S6	0.53 ± 0.31	10.39 ± 5.75	89.36 ± 10.93
S7	0.71 ± 0.11	7.33 ± 2.66	72.38 ± 16.24
S8	0.72 ± 0.09	6.90 ± 2.57	73.37 ± 11.43
S9	0.68 ± 0.09	6.64 ± 1.77	66.74 ± 20.20
	Autumn models		
A1	-0.23 ± 0.25	9.03 ± 4.79	71.40 ± 34.23
A2	-0.24 ± 0.21	8.88 ± 5.22	82.15 ± 33.96
A3	0.43 ± 0.12	7.46 ± 3.06	87.98 ± 23.15
A4	0.27 ± 0.13	7.60 ± 3.13	76.04 ± 15.55

[a] The numbers are denoted as A ± σ, where A is the mean value at four calibrated sites and σ is half of the (maximum – minimum).

References

Dufrene, E., Davi, H., Francois, C., le Maire, G., Le Dantec, V., and Granier, A.: Modelling carbon and water cycles in a beech forest Part I: Model description and uncertainty analysis on modelled NEE, Ecol Model, 185, 407-436, 2005.

Murray, M. B., Cannell, M. G. R., and Smith, R. I.: Date of Budburst of fifteen Tree Species in Britain Following Climatic Warming, J Appl Ecol, 26, 693-700, 1989.